AIAA JOURNAL
Vol. 32, No. 11, November 1994

Simulation of Turbulent Fluctuations

Giovanni Mengali* and Marco Micheli†
University of Pisa, Pisa 56126, Italy

A simulation technique is used to generate three signals representing the time variation of the velocity components in turbulent flows. This technique makes use of a bank of linear filters driven by non-Gaussian white noises. The filter impulse responses are chosen so as to obtain specified second-order (spectral) characteristics at the filter outputs. Higher order moments can also be accommodated by further specifying the statistical properties of the driving noises. The signals generated in this way may be employed to solve various engineering problems such as, for example, to test the adequacy of measurement methods based on hot-wire anemometry or to obtain gust velocity components suitable for applications in flight simulators.

I. Introduction

In many situations of aeronautical interest the problem arises of generating signals that represent, in a "realistic" way, the velocity components experienced in turbulent flows. To give an example, consider modeling the atmospheric turbulence for use in flight simulators. It is well known that simulation is a tool of primary importance in analyzing aircraft handling qualities and in assessing their performance when control systems are employed. However, simulation effectiveness is highly dependent both on the "sophistication" of the mathematical model being used and on a satisfactory description of the atmospheric disturbances.

As a second example, consider the assessment of the accuracy of measurement procedures. Suppose we know the response equations of the anemometry probes and we are able to build signals incorporating the most important characteristics of the flow we want to simulate. Thinking of them as real-world signals (i.e., derived from *ideal* acquisition instruments), one could use them to assess the sensitivity of *practical* acquisition systems to calibration and probe position errors, to establish their performance as a function of the flow parameters, and to determine the accuracy of different measurement and processing procedures. Similar measurement simulations for the accuracy analysis of hot-wire procedures were used in Ref. 1. However, in this case, only the spectra of the desired velocity fluctuations were assigned in advance, whereas no control on the remaining higher order moments was available.

The classical approach to generating signals with specified spectral characteristics is to resort to linear filters driven by white Gaussian noise.[2,3] Unfortunately, this method is not adequate in the aforementioned applications because the processes we want to simulate are typically non-Gaussian. Consider, for instance, the time variations of the velocity components in a turbulent flow. The classical method provides results that, in many cases, differ from experimental measurements insofar as the signals generated exhibit third-order moments equal to zero and fourth-order moments with a fixed relationship compared with the second-order ones.

As indicated in Refs. 4 and 5, this drawback can be partially circumvented when dealing with the generation of atmospheric turbulence for flight simulators. In these papers each velocity component is obtained as the output of a nonlinear system composed of three linear filters driven by white Gaussian signals. The outputs of two of them are added together and multiplied by the output of the third one to produce $y_i(t)$, $i = 1, 2, 3$. In this way it is possible to control the fourth-order statistics of $y_i(t)$, but the third-order statistics as well as the cross correlations between $y_i(t)$ and $y_j(t)$ cannot be chosen.

In the following we propose a method employing linear filters driven by intrinsically non-Gaussian white processes. This allows us to obtain signals with given spectral characteristics and assigned moments up to the fourth order.

The paper is organized as follows. In the next section we discuss the application of our method to a one-dimensional case. Section III deals with the general three-dimensional case, and Sec. IV describes the generation of random variables with given moments up to the fourth. Our method involves parameters, the choice of which is commented upon in Sec. V. Simulation results concerning two applications are illustrated in Sec. VI. Finally, conclusions are drawn in Sec. VII.

II. One-Dimensional Problem

Consider a sequence (a_i) of zero-mean and independent random variables (RV), all with the same density function (DF). We form the following process:

$$y(t) \triangleq \sum_{i=-\infty}^{\infty} a_i \cdot h(t - i\Delta t - \theta) \tag{1}$$

where $h(t)$ is a real-valued function of t (time), Δt is a parameter, and θ is an RV, independent of (a_i) and uniformly distributed over the interval $[0, \Delta t]$. Clearly, $y(t)$ can be viewed as the output of a linear filter, with impulse response $h(t)$, driven by

$$x(t) = \sum_{i=-\infty}^{\infty} a_i \cdot \delta(t - i\Delta t - \theta) \tag{2}$$

where $\delta(t)$ is the Dirac function.

The second-order characteristics of $y(t)$ are evaluated as follows. Define the expectations:

$$E\left[(a_i)^m\right] \triangleq A_m \qquad \forall i \in \mathbf{Z}; \qquad m = 1, 2, 3, 4 \tag{3}$$

Note that, by assumption,

$$E(a_i) = A_1 = 0 \qquad \forall i \in \mathbf{Z} \tag{4}$$

so that $y(t)$ is a zero-mean process. Also, it can be shown (see Appendix A) that the autocorrelation function of $y(t)$ is given by the following convolution:

$$R_{yy}(\tau) = \frac{A_2}{\Delta t} \int_{-\infty}^{\infty} h(t) \cdot h(t + \tau)\, dt \tag{5}$$

Thus, taking the Fourier transform of Eq. (5), we get the spectral density of $y(t)$ in the form

$$S_{yy}(f) = \frac{A_2}{\Delta t} |H(f)|^2 \tag{6}$$

Received Nov. 12, 1993; revision received May 1, 1994; accepted for publication May 6, 1994.

*Assistant Professor, Department of Aerospace Engineering, Via Diotisalvi 2.

†Graduate Student, Department of Aerospace Engineering, Via Diotisalvi 2.

with

$$H(f) = \int_{-\infty}^{\infty} h(\tau) \exp(-j2\pi f\tau)\, d\tau \tag{7}$$

Next, we concentrate on the m-order moments of $y(t)$, say $E[y^m(t)]$. Since $y(t)$ has zero mean, the first-order moment is zero. Also, $E[y^2(t)]$ is obtained from Eq. (5) by setting $\tau = 0$:

$$E[y^2(t)] = \frac{A_2}{\Delta t} \int_{-\infty}^{\infty} h^2(t)\, dt \tag{8}$$

In view of the concepts to be found in Appendix A, it is easily seen that, when m is odd, one has

$$E[y^m(t)] = \frac{A_m}{\Delta t} \int_{-\infty}^{\infty} h^m(t)\, dt \qquad m = 3, 5, 7, \ldots \tag{9}$$

When m is even, the result is more complicated. In particular, when $m = 4$ we find (see Appendix B)

$$E[y^4(t)] = \frac{A_4 - 3A_2^2}{\Delta t} \int_{-\infty}^{\infty} h^2(t)\, dt + \frac{3A_2^2}{\Delta t} \int_{-\infty}^{\infty} h^2(t) \cdot \left[\sum_{k=-\infty}^{+\infty} h^2(t - k\Delta t) \right] dt \tag{10}$$

We are now in a position to make certain remarks about these results. When $H(f) = 1$, Eq. (6) gives the spectral density of $x(t)$. Thus, $x(t)$ is white. Also, the problem of finding $H(f)$ so as to obtain a given $S_{yy}(f)$ is solved by setting $A_2 = \Delta t$, in Eq. (6), and choosing $H(f) = \sqrt{S_{yy}(f)}e^{j\varphi(f)}$, with $\varphi(f)$ arbitrary.[6] Finally, the particular structure of $x(t)$ allows us to relate the moments of $y(t)$ to the statistical properties of (a_i) through Eqs. (8–10). In other words, we can arbitrarily assign the spectral density of $y(t)$ and the moments of $y(t)$, up to the fourth-order, by making the proper choice of the statistical properties of (a_i).

III. Three-Dimensional Case

In the three-dimensional case we look for three zero-mean processes $y_1(t)$, $y_2(t)$, and $y_3(t)$ with a given covariance matrix $R(\tau)$ and specified third- and fourth-order principal moments $E[y_i^3(t)]$ and $E[y_i^4(t)]$ $(i = 1, 2, 3)$. To this end we use three independent white processes $x_1(t)$, $x_2(t)$, and $x_3(t)$, each in the form of Eq. (2), as inputs to a linear system with a transfer matrix $\mathcal{H}(f)$. This matrix must be chosen so that outputs $y_1(t)$, $y_2(t)$, and $y_3(t)$ have an assigned spectral matrix.

To proceed, let us call $[a_i^{(1)}]$, $[a_i^{(2)}]$, and $[a_i^{(3)}]$ the sequences corresponding to the processes $x_1(t)$, $x_2(t)$, or $x_3(t)$ [see Eq. (2)] and set $A_2^{(1)} = A_2^{(2)} = A_2^{(3)} = \Delta t$. This position makes the input spectral matrix an identity matrix, and the problem of finding $\mathcal{H}(f)$ so as to meet the specifications concerning the output spectral matrix has a well-known solution.[2,3] On the basis of the concepts contained in Ref. 3, we choose $\mathcal{H}(f)$ as an upper-triangular matrix, i.e.,

$$\mathcal{H}(f) = \begin{pmatrix} H_{11} & H_{12} & H_{13} \\ 0 & H_{22} & H_{23} \\ 0 & 0 & H_{33} \end{pmatrix} \tag{11}$$

and we generate $y_1(t)$, $y_2(t)$, and $y_3(t)$ as indicated in Fig. 1. The reader is referred to Ref. 3 for an in-depth discussion of this problem and the computation of $\mathcal{H}(f)$. In the following we assume that the matrix $\mathcal{H}(f)$ has already been computed.

Here we concentrate on the third- and fourth-order moments of the system output processes. For the third-order moments the following results are obtained (see Appendix C):

$$E(y_i^3) = \sum_{k=1}^{i} \frac{A_3^{(k)}}{\Delta t} \int_{-\infty}^{\infty} h_{ki}^3(t)\, dt \qquad i = 1, 2, 3 \tag{12}$$

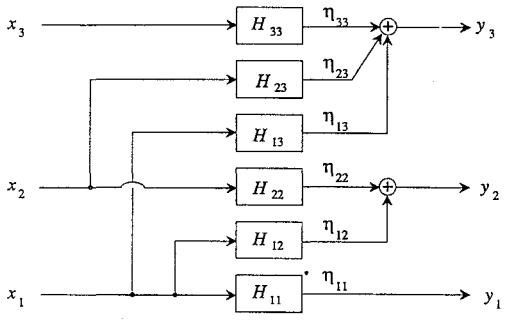

Fig. 1 Generation of three output processes.

Thus, solving Eq. (12) for the unknowns $A_3^{(i)}(i = 1, 2, 3)$ yields

$$A_3^{(1)} = \frac{E(y_1^3)}{(1/\Delta t)\int_{-\infty}^{\infty} h_{11}^3(t)\, dt} \tag{13}$$

$$A_3^{(i)} = \frac{E(y_i^3) - \sum_{k=1}^{i-1} [A_3^{(k)}/\Delta t] \int_{-\infty}^{\infty} h_{ki}^3(t)\, dt}{(1/\Delta t)\int_{-\infty}^{\infty} h_{ii}^3(t)\, dt} \qquad i = 2, 3 \tag{14}$$

Equations (13) and (14) provide relationships between the third-order moments of $a_i^{(k)}$ $(k = 1, 2, 3)$, i.e., $A_3^{(1)}$, $A_3^{(2)}$, and $A_3^{(3)}$, and the desired third-order moments of the output signals, i.e., $E(y_1^3)$, $E(y_2^3)$, and $E(y_3^3)$.

For the fourth-order moments we have (see Appendix C)

$$E(y_i^4) = \sum_{k=1}^{i} f_k + 3 \sum_{\substack{j,k=1 \\ j \neq k}}^{i} g_j g_k \qquad i = 1, 2, 3 \tag{15}$$

where

$$f_k = \frac{A_4^{(k)} - 3[A_2^{(k)}]^2}{\Delta t} \int_{-\infty}^{\infty} h_{ki}^4(t)\, dt + \frac{3[A_2^{(k)}]^2}{\Delta t} \int_{-\infty}^{\infty} h_{ki}^2(t) \cdot \left[\sum_{j=-\infty}^{+\infty} h_{ki}^2(t - j\Delta t) \right] dt \tag{16}$$

$$g_k = \frac{A_2^{(k)}}{\Delta t} \int_{-\infty}^{\infty} h_{ki}^2(t)\, dt \tag{17}$$

The relationships between $A_4^{(1)}$, $A_4^{(2)}$, and $A_4^{(3)}$ and the corresponding fourth-order moments of the output signals are easily obtained from Eqs. (15–17).

It should be noted that the output cross moments are fixed once the third- and fourth moments of $a_i^{(k)}(k = 1, 2, 3)$ are assigned. Considering, for example, the third-order cross moments, we have

$$E(y_1^2 y_k) = \frac{A_3^{(1)}}{\Delta t} \int_{-\infty}^{\infty} h_{11}^2(t) h_{1k}(t)\, dt \qquad k = 2, 3 \tag{18}$$

$$E(y_1 y_k^2) = \frac{A_3^{(1)}}{\Delta t} \int_{-\infty}^{\infty} h_{11}(t) h_{1k}^2(t)\, dt \qquad k = 2, 3 \tag{19}$$

$$E(y_2^2 y_3) = \frac{A_3^{(1)}}{\Delta t} \int_{-\infty}^{\infty} h_{12}^2(t) h_{13}(t)\, dt + \frac{A_3^{(2)}}{\Delta t} \int_{-\infty}^{\infty} h_{22}^2(t) h_{23}(t)\, dt \tag{20}$$

$$E(y_2 y_3^2) = \frac{A_3^{(1)}}{\Delta t} \int_{-\infty}^{\infty} h_{12}(t) h_{13}^2(t)\, dt + \frac{A_3^{(2)}}{\Delta t} \int_{-\infty}^{\infty} h_{22}(t) h_{23}^2(t)\, dt \tag{21}$$

$$E(y_1\,y_2\,y_3) = \frac{A_3^{(1)}}{\Delta t}\int_{-\infty}^{\infty} h_{11}(t)h_{12}(t)h_{13}(t)\,dt \tag{22}$$

In other words, since we are using three independent sequences $[a_i^{(k)}]$ $(k = 1, 2, 3)$, we can only control the principal moments of the outputs. Were we interested in also controlling the third-order cross moments, we should turn the input processes into

$$x_n(t) \triangleq \sum_{i=-\infty}^{\infty}\left[a_i^{(n)} + \sum_{k=1}^{7}\beta_{kn}b_i^{(k)}\right]\cdot\delta(t - i\Delta t - \theta) \qquad n = 1, 2, 3 \tag{23}$$

where β_{ij} are real-valued parameters, and in addition to $[a_i^{(n)}]$ $(n = 1, 2, 3)$, there are now seven further independent sequences $[b_i^{(k)}]$ $(k = 1, 2, \ldots, 7)$. Relating the output moments to the input moments gives a linear system of 10 equations in 10 unknowns $A_3^{(n)}$ $(n = 1, 2, 3)$ and $B_3^{(k)}(k = 1, 2, \ldots, 7)$. The parameters β_{ij} must be chosen in such a way that the determinant of the system is different from zero.

IV. Generation of Random Variables with Given Moments

From the preceding discussion we see that, to generate $y_i(t)$ $(i = 1, 2, 3)$ with specified statistical properties, we need random sequences $[a_i^{(n)}]$ $(n = 1, 2, 3)$ with assigned moments. This may be obtained as follows. Consider the following three RV:

w_1, Gaussian with mean μ_1 and standard deviation σ_1
w_2, Gaussian with mean μ_2 and standard deviation σ_2

$$c = \begin{cases} 1 & \text{with probability } \alpha \\ 0 & \text{with probability } 1 - \alpha \end{cases}$$

where $0 \le \alpha \le 1$. We define

$$z \triangleq cw_1 + (1 - c)w_2 \tag{24}$$

The DF of z is given by

$$p(z) = \alpha\frac{1}{\sigma_1\sqrt{2\pi}}\exp\left[-(z-\mu_1)^2/2\sigma_1^2\right] + (1-\alpha)\frac{1}{\sigma_2\sqrt{2\pi}}\exp\left[-(z-\mu_2)^2/2\sigma_2^2\right] \tag{25}$$

We want to determine α, μ_1, μ_2, σ_1, and σ_2 so that z has zero mean and given second-, third- and fourth-order moments (say, m_2, m_3, and m_4).

It is easy to establish that this requires:

$$\begin{aligned} \alpha\mu_1 + (1-\alpha)\mu_2 &= 0 \\ \alpha\left(\sigma_1^2 + \mu_1^2\right) + (1-\alpha)\left(\sigma_2^2 + \mu_2^2\right) &= m_2 \\ \alpha\left(3\sigma_1^2\mu_1 + \mu_1^3\right) + (1-\alpha)\left(3\sigma_2^2\mu_2 + \mu_2^3\right) &= m_3 \\ \alpha\left(3\sigma_1^4 + 6\sigma_1^2\mu_1^2 + \mu_1^4\right) + (1-\alpha)\left(3\sigma_2^4 + 6\sigma_2^2\mu_2^2 + \mu_2^4\right) &= m_4 \end{aligned} \tag{26}$$

These equations may be rearranged as

$$\mu_1^3\left(\frac{1+\alpha}{3(1-\alpha)} - 1\right) + \mu_1 \times\sqrt{\left(m_4 - 3m_2^2\right)\frac{1-\alpha}{3\alpha} + \mu_1^4\frac{2 - 6\alpha + 6\alpha^2}{3(1-\alpha)^2}} - m_3\frac{1-\alpha}{3\alpha} = 0 \tag{27}$$

$$\sigma_1^2 = m_2 - \mu_1^2 + \sqrt{\left(m_4 - 3m_2^2\right)\frac{1-\alpha}{3\alpha} + \mu_1^4\frac{2-6\alpha+6\alpha^2}{3(1-\alpha)^2}} \tag{28}$$

$$\sigma_2^2 = \left(m_2 - \alpha\sigma_1^2 - \frac{\alpha}{1-\alpha}\mu_1^2\right)\cdot\frac{1}{1-\alpha} \tag{29}$$

$$\mu_2 = \frac{\alpha}{1-\alpha}\mu_1 \tag{30}$$

and may then be solved in cascade as follows.

When $m_4 \ge 3m_2^2$ (which is a reasonable hypothesis when dealing with problems involving turbulence fields), it can be checked that Eq. (27) has (at least) one solution $\mu_1 = \mu_1(\alpha)$ for any $0 \le \alpha \le 1$. One would be tempted to insert such a solution into Eq. (28) to get σ_1, then to insert μ_1 and σ_1 into Eq. (29) to obtain σ_2, and finally to insert μ_1 into Eq. (30) to get μ_2. Unfortunately, this process might fail because the right-hand sides of Eq. (28) or Eq. (29) might be negative. So, one wonders how α may be chosen to avoid this difficulty. In this connection it can be shown that if

$$m_4 \ge m_2^2 + \frac{m_3^2}{m_2} \tag{31}$$

then the previous solution process does work if α is close to

$$\bar{\alpha} = \frac{1}{2}\cdot\left[1 - \frac{1}{\sqrt{1 + 4\left(m_2^3/m_3^2\right)}}\right] \tag{32}$$

In particular, $\alpha = \bar{\alpha}$ turns out to be the only solution for Eq. (26) when equality holds true in Eq. (31).

From the previous discussion we see that there is some flexibility in the values of μ_1, μ_2, σ_1, and σ_2 that we can obtain. In other words, some control is allowed on the moments greater than four with a proper choice of α.

V. Choice of the Parameters for Signal Generation

Now we return to the one-dimensional problem. It has been previously shown that processes $x(t)$ and $y(t)$ depend on parameters Δt and θ [see Eqs. (1) and (2)]. In the following we give guidelines for the choice of such parameters. Basically, the idea is that θ can be chosen arbitrarily provided Δt is small enough. To prove this claim we consider the fourth-order moment $E(y^4 \mid \theta)$ and show that it is independent of θ when $1/\Delta t \ge 4B$, where B is the bandwidth of filter $h(t)$. It is not hard to see that, on the basis of these assumptions, the lower order moments are also independent of θ.

From Appendix D we have

$$E(y^4 \mid \theta) = \frac{A_4 - 3A_2^2}{\Delta t}\sum_{n=-\infty}^{\infty} H_4\left(\frac{n}{\Delta t}\right) \cdot\exp[j\cdot 2\pi\cdot(t-\theta)(n/\Delta t)] + 3A_2^2\left[\frac{1}{\Delta t}\sum_{n=-\infty}^{\infty} H_2\left(\frac{n}{\Delta t}\right)\cdot\exp[j\cdot 2\pi\cdot(t-\theta)(n/\Delta t)]\right]^2 \tag{33}$$

where $H_m(f)(m = 2, 4)$ is the Fourier transform of $h^m(t)$. By definition, the bandwidth B of $h(t)$ is such that

$$H(f) = 0 \text{ for } |f| \ge B \tag{34}$$

Clearly, the bandwidths of $H_2(f)$ and $H_4(f)$ are $B_2 = 2B$ and $B_4 = 4B$, respectively. Assuming

$$\frac{1}{\Delta t} > 4B \tag{35}$$

we see that all of the terms in summations (33) vanish except for those with index $n = 0$. In these conditions, Eq. (33) reduces to

$$E(y^4 \mid \theta) = \frac{A_4 - 3A_2^2}{\Delta t}H_4(0) + 3A_2^2\left[\frac{H_2(0)}{\Delta t}\right]^2 \tag{36}$$

which shows that $E(y^4 \mid \theta)$ is independent of θ. In other words, if Δt is chosen according to Eq. (35), θ can be arbitrarily set, and, in particular, we can put $\theta = 0$. In this case Eq. (1) becomes

$$y(t) = \sum_{i=-\infty}^{\infty} a_i \cdot h(t - i\Delta t) \tag{37}$$

Indeed, we used Eq. (37) to generate the signals in the simulations.

VI. Simulation Results

A. Simulation of a Turbulent Flow at the Outlet of a Coaxial Jet

In this example we used the data obtained from experimental measurements of flow velocity at the outlet of two free coaxial jets.[7,8] Time histories of the components of the flow velocities were recorded at 6000 samples per second. Each acquisition lasted 65,536 samples. The measurements were made for $x/D_i = 3.5$ and $y/D_i = 0.75$ in the graphs in Figs. 2 and 3. Such measurements provided information about 1) the components of the Reynolds tensor, 2) the spectral matrix of the velocity components u and v, 3) estimates of their density functions, and 4) their central moments up to the fourth order. Since no information was available about the third fluctuating velocity component w, it was decided to put $w = v$. Moreover, the cross spectra of the pairs (u, w) and (v, w) were arbitrarily set to zero. Finally, the first velocity component was generated with a unity mean square value.

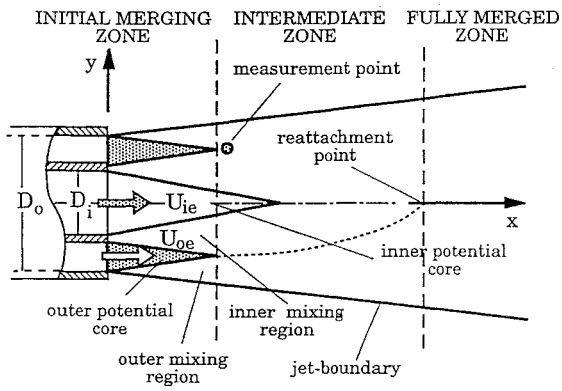

Fig. 2 Flowfield of a typical coaxial jet configuration (see Ref. 7).

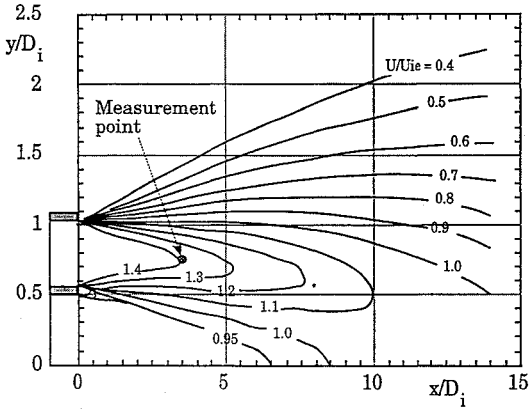

Fig. 3 Isocontours of mean axial velocity normalized to internal exit velocity, U_{ie} (see Ref. 7).

Table 1 Comparison between assigned and obtained results for the Reynolds tensor

Assigned Reynolds tensor			Obtained Reynolds tensor		
1.0	0.1941	0	1.0085	0.1968	−0.0066
0.1941	1.1827	0	0.1968	1.1782	−0.0035
0	0	1.1827	−0.0066	−0.0035	1.1782

The assigned components of the Reynolds tensor are as follows:

$$\mathrm{Re}(x/D_i = 3.5,\ y/D_i = 0.75) = \begin{pmatrix} 1.0 & 0.1941 & 0 \\ 0.1941 & 1.1827 & 0 \\ 0 & 0 & 1.1827 \end{pmatrix} (\mathrm{m}^2/\mathrm{s}^2)$$

The signals (each 581,632 samples long) were generated at a sampling rate of 6000 Hz. Results are shown in Tables 1 and 2. They indicate that the simulation method works very well since the differences between the actual and the desired values of the various moments are smaller than the measurement errors achievable by standard instrumentation.

The spectra of the signals generated are compared with the corresponding assigned spectra in Figs. 4–7. Spectral estimates were made by means of the Welch method by grouping the samples in 567 blocks, each of 2048 samples.

The time histories of the actual and simulated u components are shown in Fig. 8. Finally, Figs. 9 and 10 show density functions for u and v, as obtained from the data records and from the simulated signals. The agreement between measured and simulated signals is remarkable. For comparison purposes, a Gaussian DF is also indicated, with a variance equal to the measured signal mean square value. It should be stressed that the measured/simulated distributions are not Gaussian. Indeed, it is clear from Table 2 that u, v, and w all have third-order moments that are quite different from zero.

B. Generation of Gust-Induced Velocity Components

As a second example, the velocity component in an atmospheric turbulence field was simulated. A Dryden spectrum with a turbulence scale length of 533 m was used. Figure 11 shows the assigned spectrum along with that obtained by simulation. Also, Fig. 12 illustrates the DF of the simulated signal and compares it with the DF

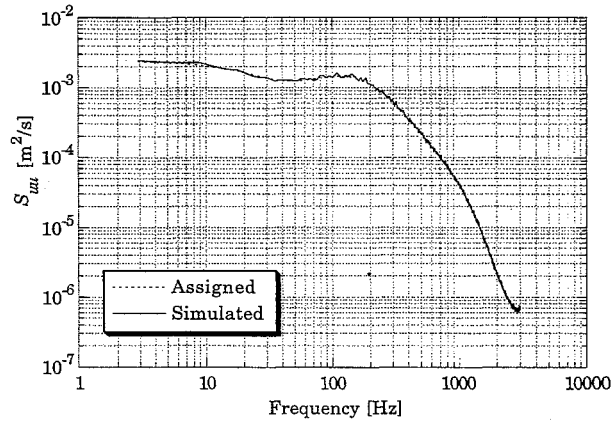

Fig. 4 Comparison between assigned and simulated spectra (u component).

Table 2 Comparison between assigned and obtained results for the third- and fourth-order moments

Third-order principal moments			Fourth-order principal moments		
Notation	Assigned value	Obtained value	Notation	Assigned value	Obtained value
$\overline{uuu}$	−1.3687	−1.3963	$\overline{uuuu}$	6.9964	7.1620
$\overline{vvv} = \overline{www}$	−0.6764	−0.6547	$\overline{vvvv} = \overline{wwww}$	5.6536	5.5475

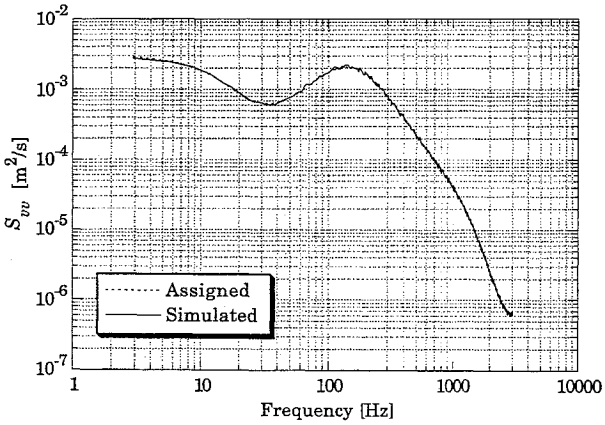

Fig. 5 Comparison between assigned and simulated spectra (v component).

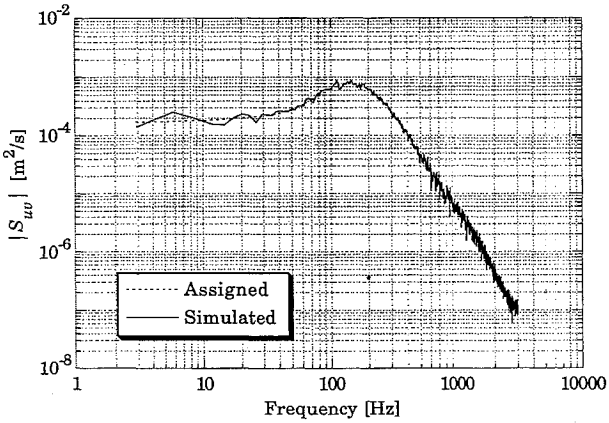

Fig. 6 Comparison between assigned and simulated u, v cross spectra (amplitude).

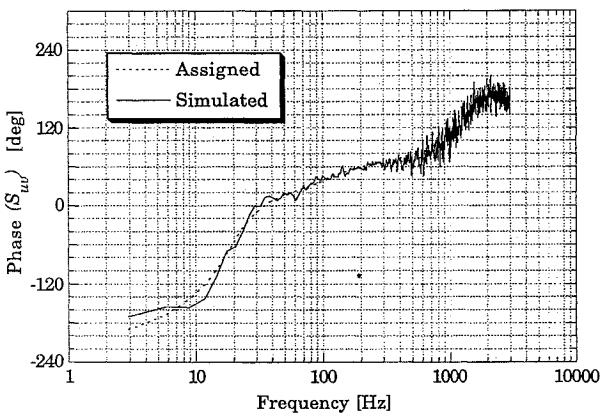

Fig. 7 Comparison between assigned and simulated u, v cross spectra (phase).

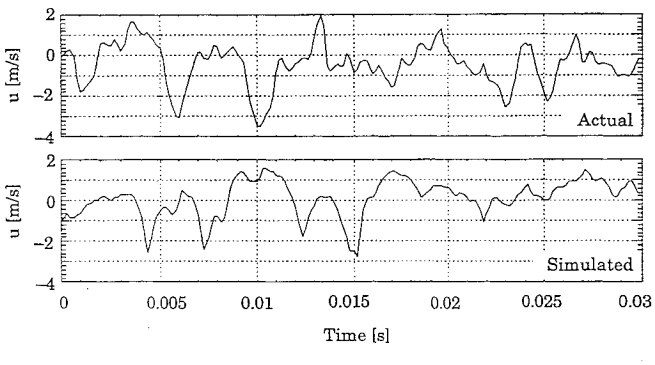

Fig. 8 Time histories of the actual and simulated u component.

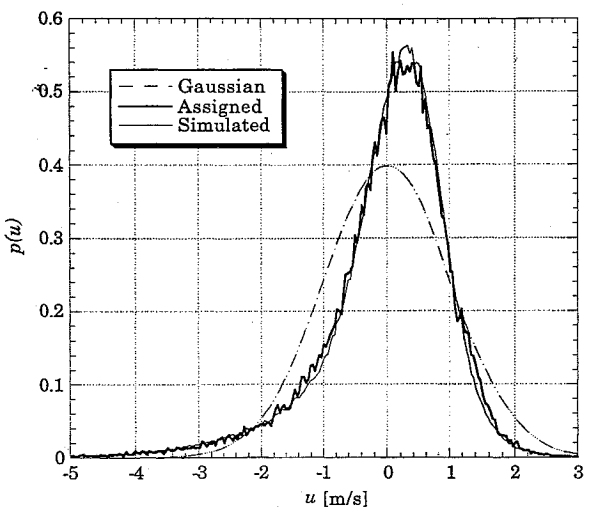

Fig. 9 Comparison between assigned and simulated density functions for the u component.

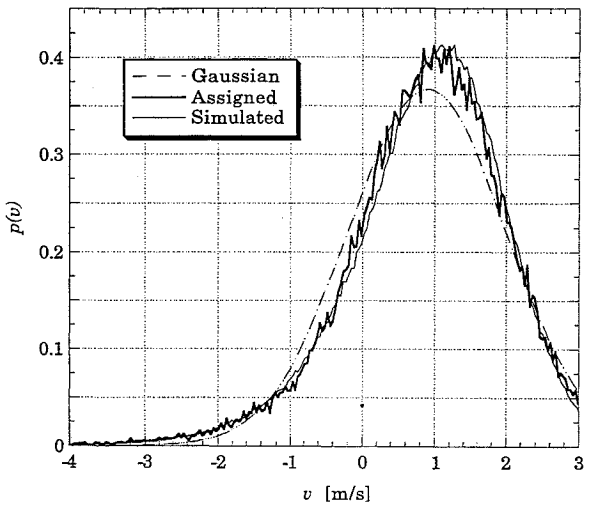

Fig. 10 Comparison between assigned and simulated density functions for the v component.

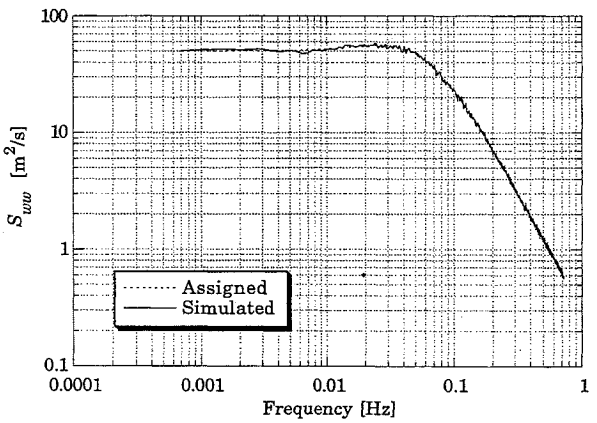

Fig. 11 Comparison between assigned (Dryden) and simulated spectra.

of a Gaussian signal with the same mean square value. Note that the simulated signal has a kurtosis value equal to 5.5, whereas its skewness is zero.

In Fig. 13, the time histories of the simulated signal and of a Gaussian signal are compared; also given are the time histories of the squares of these signals. The burstlike nature of the non-Gaussian signal should be noted; this is a well-known feature of atmospheric turbulence, which must be reproduced in the sim-

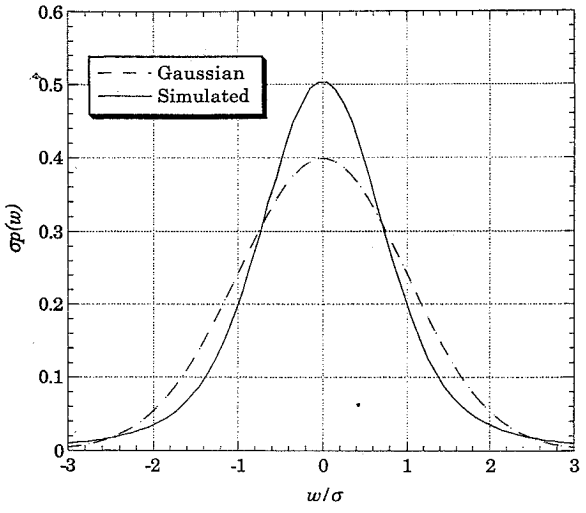

Fig. 12 Comparison between Gaussian and simulated density functions for the w component.

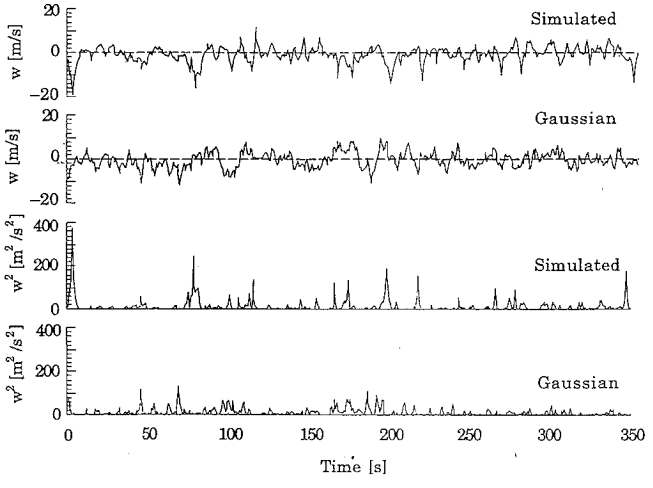

Fig. 13 Time histories of a Gaussian and a non-Gaussian (kurtosis = 5.5) velocity component along with the signal squares.

ulations to obtain realistic time histories. This is of paramount importance in the implementation of flight simulators because, in general, pilots feel Gaussian turbulence is too "regular" to be realistic.

VII. Conclusions

We have examined the problem of generating signals with given spectral characteristics *and* assigned higher order moments (up to the fourth). To this end, a bank of linear filters is used, whose inputs are non-Gaussian white noises. The filter impulse responses are chosen on the basis of the spectral properties of the signals we want to generate. The specifications on the third- and fourth-order moments are met by generating sequences of zero mean independent RV with specified standard deviation, skewness, and kurtosis.

The signals generated in this way may be used to represent the random velocity components in turbulent flows. Also, they have interesting applications in practical situations where a Gaussian signal model is not adequate. Two applications have been described, consisting of the simulation of a turbulent flow at the outlet of a coaxial jet and of a velocity component in an atmospheric turbulent field.

The results demonstrate that non-Gaussian signals with given statistical properties can be simulated with a high degree of accuracy.

Appendix A

From Eq. (1) we have:

$$E[y(t+\tau)y(t) \mid \theta]$$

$$= E\left[\sum_{i=-\infty}^{\infty}\sum_{k=-\infty}^{\infty} a_i a_k h(t+\tau-i\Delta t-\theta)\cdot h(t-k\Delta t-\theta)\right]$$

$$= A_2\sum_{i=-\infty}^{\infty} h(t+\tau-i\Delta t-\theta)\cdot h(t-i\Delta t-\theta) \tag{A1}$$

In obtaining Eq. (A1), we made use of the linearity of $E(\cdot)$ and of the fact that

$$E(a_i a_j) = \begin{cases} A_2 & \text{for } i=j \\ 0 & \text{otherwise} \end{cases} \tag{A2}$$

Averaging Eq. (A1) over θ and bearing in mind that θ is uniformly distributed over $[0, \Delta t]$, we have

$$E[y(t+\tau)y(t)]$$

$$= \frac{A_2}{\Delta t}\sum_{i=-\infty}^{\infty}\int_0^{\Delta t} h(t-i\Delta t-\theta)\cdot h(t+\tau-i\Delta t-\theta)\,d\theta \tag{A3}$$

from which, substituting $\xi = t - i\Delta t - \theta$, we obtain

$$E[y(t+\tau)y(t)] = \frac{A_2}{\Delta t}\sum_{i=-\infty}^{\infty}\int_{t-(i+1)\Delta t}^{t-i\Delta t} h(\xi)\cdot h(\xi+\tau)\,d\xi \tag{A4}$$

and finally

$$E[y(t+\tau)y(t)] = R_{yy}(\tau) = \frac{A_2}{\Delta t}\int_{-\infty}^{\infty} h(t)\cdot h(t+\tau)\,dt \tag{A5}$$

which proves Eq. (5).

A final remark is necessary. From Eqs. (A1) and (A5) we see that, whereas $E[y(t+\tau)y(t) \mid \theta]$ is a function of time, $E[y(t+\tau)y(t)]$ is not. This motivates the introduction of θ in Eq. (1) so as to obtain a wide-sense stationary process.

Appendix B

Making use of Eq. (1) we have

$$E(y^4 \mid \theta) = E\left[\sum_{i,j,k,n=-\infty}^{\infty} a_i a_j a_k a_n h(t-i\Delta t-\theta)\right.$$

$$\left.\times h(t-j\Delta t-\theta)h(t-k\Delta t-\theta)h(t-n\Delta t-\theta)\right] \tag{B1}$$

On the other hand

$$E(a_i a_j a_k a_n) = \begin{cases} A_4 & i=j=k=n \\ & i=j \text{ and } k=n \text{ but } i\neq k \\ A_2^2 & i=k \text{ and } j=n \text{ but } i\neq j \\ & i=n \text{ and } j=k \text{ but } i\neq j \\ 0 & \text{otherwise} \end{cases}$$

so that

$$E[y^4(t) \mid \theta] = A_4\sum_{i=-\infty}^{\infty} h^4(t-i\Delta t-\theta)$$

$$+3A_2^2\sum_{i=-\infty}^{\infty} h^2(t-i\Delta t-\theta)\sum_{\substack{k=-\infty \\ i\neq k}}^{\infty} h^2(t-k\Delta t-\theta)$$

$$= \left(A_4 - 3A_2^2\right)\sum_{i=-\infty}^{\infty} h^4(t-i\Delta t-\theta)$$

$$+3A_2^2\sum_{i=-\infty}^{\infty}\sum_{k=-\infty}^{\infty} h^2(t-i\Delta t-\theta)h^2(t-k\Delta t-\theta) \tag{B2}$$

Averaging over θ,

$$E[y^4(t)] = \frac{A_4 - 3A_2^2}{\Delta t} \sum_{i=-\infty}^{\infty} \int_0^{\Delta t} h^4(t - i\Delta t - \theta)\, d\theta + \frac{3A_2^2}{\Delta t} \sum_{i=-\infty}^{\infty} \sum_{k=-\infty}^{\infty} \int_0^{\Delta t} h^2(t - i\Delta t - \theta) h^2(t - k\Delta t - \theta)\, d\theta \tag{B3}$$

and using the substitution $\xi = t - i\Delta t - \theta$, we obtain

$$E\left[y^4(t)\right] = \frac{A_4 - 3A_2^2}{\Delta t} \sum_{i=-\infty}^{\infty} \int_{t-(i+1)\Delta t}^{t-i\Delta t} h^4(\xi)\, d\xi + \frac{3A_2^2}{\Delta t} \sum_{i=-\infty}^{\infty} \int_{t-(i+1)\Delta t}^{t-i\Delta t} \left\{ h^2(\xi) \sum_{k=-\infty}^{\infty} h^2[\xi + (i-k)\Delta t] \right\} d\xi \tag{B4}$$

Next, observe that

$$\sum_{k=-\infty}^{\infty} h^2[\xi + (i-k)\Delta t] = \sum_{k=-\infty}^{\infty} h^2[\xi - k\Delta t] \tag{B5}$$

i.e., the sum over k is invariant with respect to a time shift proportional to Δt. Hence, from Eq. (B4) we get

$$E[y^4(t)] = \frac{A_4 - 3A_2^2}{\Delta t} \int_{-\infty}^{\infty} h^4(t)\, dt + \frac{3A_2^2}{\Delta t} \int_{-\infty}^{\infty} h^2(t) \cdot \left[\sum_{k=-\infty}^{+\infty} h^2(t - k\Delta t) \right] dt$$

which proves Eq. (10).

Appendix C

From Fig. 1, using * for the convolution, we have

$$y_i = \sum_{k=1}^{i} h_{ki} * x_k = \sum_{k=1}^{i} \eta_{ki} \qquad i = 1, 2, 3 \tag{C1}$$

from which we obtain

$$y_i^3 = \sum_{k=1}^{i} \eta_{ki}^3 + 3 \sum_{\substack{j,k=1 \\ j \neq k}}^{i} \eta_{ji}^2 \eta_{ki} + 6 \sum_{\substack{j,k,n=1 \\ j \neq k \neq n}}^{i} \eta_{ji} \eta_{ki} \eta_{ni} \qquad i = 1, 2, 3 \tag{C2}$$

Bearing in mind that the input processes are mutually independent and zero mean, we get

$$E\left(\eta_{ji}^2 \eta_{ki}\right) = E(\eta_{ji} \eta_{ki} \eta_{ni}) = 0 \tag{C3}$$

so that

$$E\left(y_i^3\right) = \sum_{k=1}^{i} E\left(\eta_{ki}^3\right) \qquad i = 1, 2, 3 \tag{C4}$$

Reasoning as in Eq. (9), we immediately find

$$E\left(\eta_{ki}^3\right) = \frac{A_3^{(k)}}{\Delta t} \int_{-\infty}^{\infty} h_{ki}^3(t)\, dt \qquad i = 1, 2, 3 \tag{C5}$$

which proves Eq. (12).

In a similar way we have

$$y_i^4 = \sum_{k=1}^{i} \eta_{ki}^4 + 3 \sum_{\substack{j,k=1 \\ j \neq k}}^{i} \eta_{ji}^2 \eta_{ki}^2 + 4 \sum_{\substack{j,k=1 \\ j \neq k}}^{i} \eta_{ji}^3 \eta_{ki} + 6 \sum_{\substack{j,k,n=1 \\ j \neq k \neq n}}^{i} \eta_{ji}^2 \eta_{ki}, \eta_{ni} \qquad i = 1, 2, 3 \tag{C6}$$

On the other hand

$$E\left(\eta_{ji}^3 \eta_{ki}\right) = E\left(\eta_{ji}^2 \eta_{ki} \eta_{ni}\right) = 0 \tag{C7}$$

so that

$$E\left(y_i^4\right) = \sum_{k=1}^{i} E\left(\eta_{ki}^4\right) + 3 \sum_{\substack{j,k=1 \\ j \neq k}}^{i} E\left(\eta_{ji}^2\right) E\left(\eta_{ki}^2\right) \qquad i = 1, 2, 3 \tag{C8}$$

from which Eqs. (15–17) follow, bearing in mind Eqs. (8) and (10).

Appendix D

From Eq. (A1), substituting $k = -i$, we obtain

$$E(y^4 \mid \theta) = \left(A_4 - 3A_2^2\right) \sum_{k=-\infty}^{\infty} h^4(k\Delta t + t - \theta) + 3A_2^2 \left[\sum_{k=-\infty}^{\infty} h^2(k\Delta t + t - \theta) \right]^2 \tag{D1}$$

This equation can be rearranged in a more useful form by using the Poisson summation formula[9] that holds true for any $h(t)$ with Fourier transform $H(f)$

$$\sum_{k=-\infty}^{\infty} h(k \cdot \Delta t) = \frac{1}{\Delta t} \sum_{n=-\infty}^{\infty} H\left(\frac{n}{\Delta t}\right) \tag{D2}$$

Making use of Eq. (D2), Eq. (D1) is transformed into Eq. (33).

Acknowledgment

The authors are greatly indebted to Guido Buresti for his encouragement and for his suggestions concerning hot-wire anemometry.

References

[1]Buresti, G., and Di Cocco, N. R., "Hot-Wire Measurement Procedures and Their Appraisal Through a Simulation Technique," *Journal of Physics E: Scientific Instruments*, Vol. 20, 1987, pp. 87–99.

[2]Dodds, C. J., and Robson, J. D., "Partial Coherence in Multivariate Random Processes," *Journal of Sound and Vibration*, Vol. 42, No. 2, 1975, pp. 243–249.

[3]Bendat, J. S., and Piersol, A. G., *Engineering Applications of Correlation and Spectral Analysis*, Wiley, New York, 1980, pp. 259–263.

[4]Van de Moesdijk, G. A. J., "The Description of Patchy Atmospheric Turbulence, Based on a Non-Gaussian Simulation Technique," Technical Univ. of Delft, Rept. VTH-192, The Netherlands, Feb. 1975.

[5]Baarspul, M., "Mathematical Modelling of Flight in Turbulence and Windshear," Technical Univ. of Delft, Rept. LR-600, The Netherlands, Oct. 1989.

[6]Papoulis, A., *Probability, Random Variables and Stochastic Processes*, McGraw-Hill, New York, 1965, pp. 347–350.

[7]Buresti, G., Mordacci, A., Petagna, P., Talamelli, A., and Tanzini, G., "Experimental Analysis of Coaxial Jets by Means of Computer Aided Data Acquisition and Processing," *Computational Methods and Experimental Measurements VI*, Vol. 1, Heat and Fluid Flow, edited by C. A. Brebbia and G. M. Carlomagno, CMP & Elsevier Applied Science, 1993, pp. 247–262.

[8]Buresti, G., Mordacci, A., Petagna, P., Talamelli, A., and Tanzini, G., "Experimental Analysis of the Turbulent Field of a Coaxial Jet Configuration," *Engineering Turbulence Modelling and Experiments 2*, edited by W. Rodi and F. Martelli, Elsevier, 1993, pp. 457–466.

[9]Ziemer, R. E., Tranter, W. H., and Fannin, D. R., *Signals and Systems, Continuous and Discrete*, Macmillan, 1983.